Dyes and Pigments 148 (2018) 81–90

Contents lists available at ScienceDirect

Dyes and Pigments

journal homepage: www.elsevier.com/locate/dyepig

Improved synthesis of tetraaryl-1,4-dihydropyrrolo[3,2-*b*]pyrroles a promising dye for organic electronic devices: An experimental and theoretical approach

Lucas Michelão Martins [a], Samuel de Faria Vieira [b], Gabriel Baldo Baldacim [a], Bruna Andressa Bregadiolli [a], José Cláudio Caraschi [b], Augusto Batagin-Neto [b], Luiz Carlos da Silva-Filho [a, *]

[a] Laboratory of Organic Synthesis and Processes, Department of Chemistry, São Paulo State University (UNESP) – School of Sciences, Av. Eng. Luiz Edmundo Carrijo Coube, 14-01, 17033-360 Bauru, SP, Brazil
[b] São Paulo State University (UNESP), Campus Itapeva, Rua Geraldo Alckmin, 519, 18409-010 Itapeva, SP, Brazil

ARTICLE INFO

Article history:
Received 13 June 2017
Received in revised form
14 August 2017
Accepted 30 August 2017
Available online 1 September 2017

Keywords:
Niobium pentachloride
Heterocycles
Fluorescence
Multicomponent reactions
Density functional calculations

ABSTRACT

Pyrrolo-[3,2-*b*]pyrroles represent a class of promising materials for application in organic electronics with interesting optoelectronic properties and great synthesis versatility, but yields obtained from varied synthetic routes are still very low, hindering their effective application for industrial purposes. In this report, we present a method for the synthesis of tetraaryl-1,4-dihydropyrrolo-[3,2-*b*]pyrrole derivatives by multicomponent reactions employing niobium pentachloride as a catalyst. The optical characterization of the products is also presented. Electronic structure calculations were performed to help the interpretation of the synthesis process, as well as the optical properties of the systems. Excellent yields and low reaction times were obtained, indicating that $NbCl_5$ is an efficient catalyst for such systems. The products show promising properties for optoelectronic applications that can be adjusted by the choice of benzaldehyde derivatives used in the synthesis.

1. Introduction

Heteropentalenes belong to a class of heterocyclic compounds with two fused pentagonal rings [1]. Derivatives with 10 π electrons are aromatic and have been studied due to their potential use in electronic devices, such as solar cells [2], transistors [3], and electrochromic devices [4,5]. Among the aromatic heteropentalenes, those most frequently studied are the thieno[3,2-*b*]thiophenes and thieno[3,2-*b*]pyrroles [3,4,6–12].

In this context, dihidropyrrolo-[3,2-*b*]pyrrole derivatives have gained increasing attention in recent years, mainly because of their high fluorescence quantum yields and significant two-photon absorption (2PA) cross-sections [13–15]. In addition, the pyrrolo[3,2-*b*]pyrrole structure has also been predicted as the most efficient electron donor among the 10 π electron systems, such as thieno[3,2-*b*]thiophene and thieno[3,2-*b*]pyrrole [16]. Regarding optical properties, it has been shown that some azapentalene derivatives present very broad absorption spectra presenting colorations ranging from blue to red [17–19].

Some works also show that the tetraaryl-1,4-dihydropyrrolo-[3,2-*b*]pyrrole derivatives can be used as starting materials to synthesize other electron-rich structures, including pentaaryl- and hexaaryl-1,4-dihydropyrrolo-[3,2-*b*]pyrroles, diindolo[2,3-b:2′,3′-f]pyrrolo[3,2-*b*]pyrroles, bis(areno)-1,4-dihydropyrrolo[3,2-*b*]pyrroles and π-expanded indolo[3,2-*b*]indoles [20–27]. Recently, the technological relevance of pyrrolo[3,2-*b*]pyrrole derivatives has been demonstrated in applications such as the halocarbon detection cartridges [28] and the organic resistive memory [29]. However, in the field of photoelectronics, the pyrrolo[3,2-*b*]pyrrole derivatives are not yet studied, but similar heteropentalenes such as thieno[3,2-*b*]thiophenes appear as dyes in dye-sensitized solar cells (DSSC) [30,31], as hole transporters in Perovskite solar cells (PSC) [32], in organic light emitting diodes (OLED) [33], organic light emitting transistors (OLET) [34], organic phototransistors (OPT) [35] and organic photovoltaic cells (OPV) [36].

Pyrrolo[3,2-*b*]pyrrole derivatives can be synthesized via

* Corresponding author.
E-mail address: lcsilva@fc.unesp.br (L.C. da Silva-Filho).

http://dx.doi.org/10.1016/j.dyepig.2017.08.056
0143-7208/

Knoevenagel reaction between pyrrolo-2-carboxialdehydes and ethyl azidoacetate, with a subsequent thermal cyclization [37]. Mukai and coworkers described the preparation of these materials in multiple steps, but showed low yields [38–40]. A new method for their preparation was reported in 2013, consisting of a domino reaction between an amine, an aldehyde and butane-2,3-dione in a 2:2:1 proportion and in glacial acetic acid at reflux. This reaction produces the desired tetraaryl-1,4-dihydropyrrolo[3,2-*b*]pyrrole derivatives; however, low yields were still obtained (5–34%) [41]. A relevant improvement in this method was reported by the same research group in 2014, adding 10 mol% of *p*-toluene sulfonic acid as a catalyst to the reaction, which led to yields between 22 and 49% [42].

Janiga and coworkers suggest that the synthesis of tetraaryl-1,4-dihydropyrrolo[3,2-*b*]pyrrole derivatives occurs by a Mannich multicomponent reaction (MCR), with *in situ* generation of a Schiff base, which suffers the attack of the enol form of the butane-2,3-dione, followed by a cyclization reaction to form an enamine intermediate. This enamine reacts with a second Schiff base, followed by another cyclization and finally an oxidation (Scheme 1) [41].

Based on such mechanistic proposal, it is possible to point out niobium pentachloride ($NbCl_5$) as a promising candidate to promote the involved pentacomponent reactions. As a matter of fact, niobium pentachloride was the only Lewis acid capable of promoting the Mannich MCR between aniline, benzaldehyde and the acetophenone derivatives at room temperature with great yields and good reaction times highlighting its powerful catalytic properties [43].

$NbCl_5$ is highly electrophilic and therefore can act as a Lewis acid, catalyzing several organic reactions and leading to excellent yields [44–51]. In particular, good results have been obtained by using this material as catalyst in several MCRs [52–61]. In this context, in the present report, we evaluate the use of $NbCl_5$ as catalyst in the synthesis of tetraaryl-1,4-dihydropyrrolo[3,2-*b*]pyrrole derivatives by the pentacomponent reaction involving benzaldehyde, aniline and β-diketone derivatives. Preliminary photophysical characterization of the obtained products was also conducted. Electronic structure calculations were carried out in order to interpret the results and also to propose derivatives with optimized opto-electronic properties.

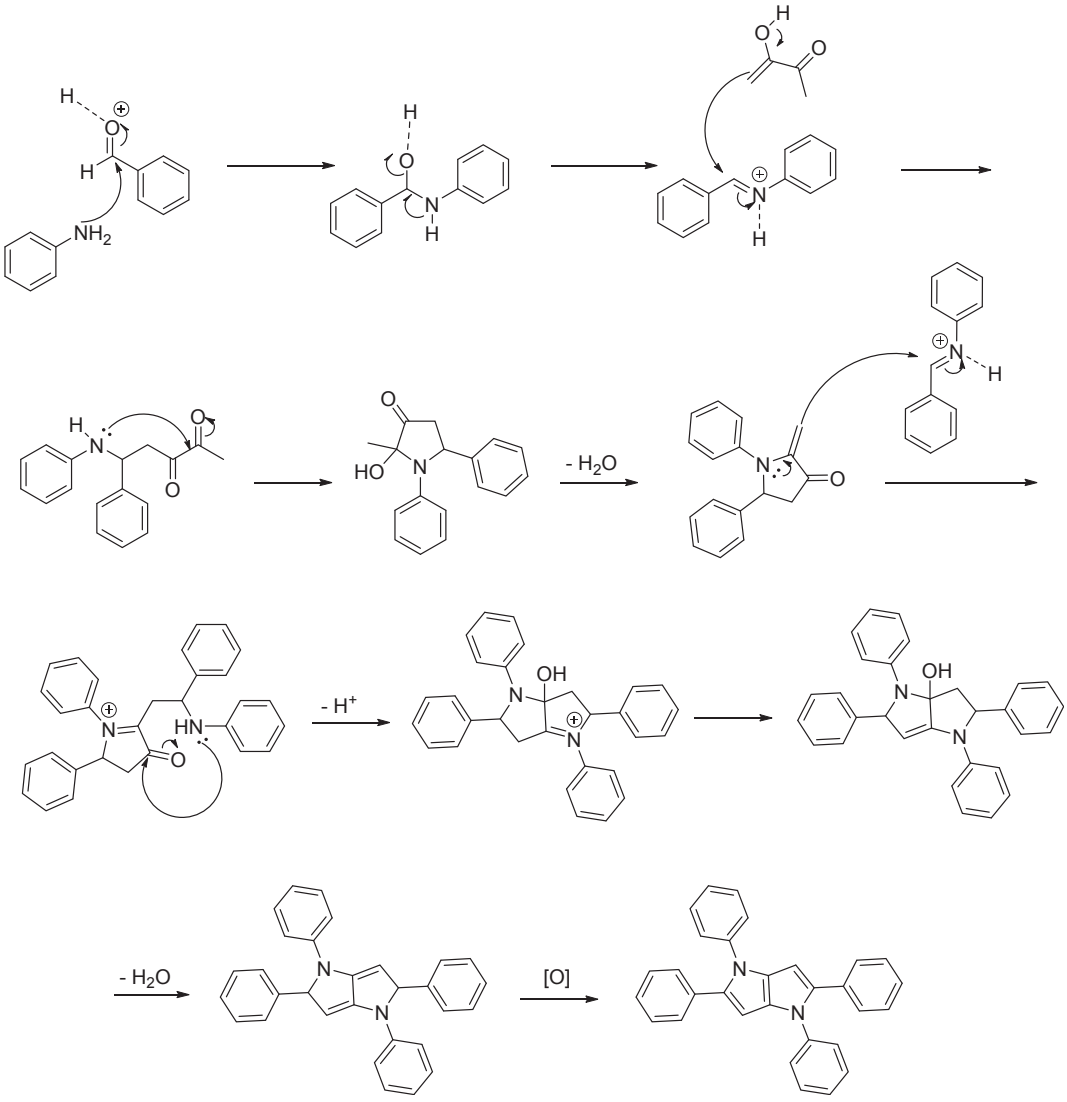

Scheme 1. Mechanistic proposal for the synthesis of tetraaryl-1,4-dihydropyrrolo[3,2-*b*]pyrrole derivatives.

2. Experimental

2.1. Materials and measurements

All reactions were performed using anhydrous acetonitrile. All of the chemicals were purchased from Sigma-Aldrich Chemical Co. (St. Louis, MO, USA) and used without further purification. Thin-layer chromatography was performed on 0.2 mm Merck 60 F_{254} silica gel aluminum sheets, which were visualized with a phosphomolybdic acid/ammonium cerium (IV) sulfate/water/sulfuric acid mixture. Bruker DRX 400 spectrometer was used for the NMR spectra ($CDCl_3$ solutions) using tetramethylsilane as internal reference for ^1H and $CDCl_3$ as an internal reference for ^{13}C. A Jasco FTIR model 4600 was used to record IR spectra (KBr pellets). HRMS analyses were recorded on micrOTOF (Bruker), with ESI-TOF detector operating on positive mode. UV–Vis spectra were recorded in an Agilent Technologies Cary 8454 and fluorescence spectra in a SpectraMax M2, from Molecular Devices, both in room temperature with a 10 mm quartz cuvette. Fluorescence emission spectra were obtained using a Synergy2 Multi-Mode reader (BioTek, USA).

Quantum yields were analyzed by adjusting the solution absorption using the UV–Vis to ca. 0.05 at 272–388 nm wavelength, the output was measured using the luminescence spectrophotometer at the same wavelength and comparing it to the known 9,10-diphenylanthracene standard using eq. (1):

$$\Phi_f = \Phi_{std} x \frac{A_{std} F}{A F_{std}} x \frac{n^2}{n_{std}^2} \quad (1)$$

Φ is the fluorescence quantum yield, A is the absorption of the excitation wavelength, F is the area under the emission curve, and n is the refractive index of the solvents used. Subscript *std* denotes the standard. The compounds were solubilized in ethanol and the concentration maintained at about $1{,}0 \times 10^{-6}$ M to follow the protocol for analysis.

2.2. Computational details

All the structures were optimized in a DFT approach employing B3LYP (Becke, three parameter, Lee-Yang-Parr) exchange-correlation functional and 6-311G(d,p) basis set. The presence of the solvent (CH_3CN) was simulated via polarizable continuum model (PCM) implemented in the Gaussian 09 computational package [62].

2.3. Synthesis

2.3.1. General procedure for the synthesis of tetraaryl-1,4-dihydropyrrolo[3,2-b]pyrrole derivatives

For a solution of niobium pentachloride (0.250 mmol) in 1.0 mL of anhydrous acetonitrile, maintained at room temperature in a capped flask, we added a solution of the benzaldehyde derivative (**1a-j**) (2.0 mmol), aniline derivative (**2a-e**) (2.0 mmol) and β-diketone (**3a-c**) (1.0 mmol) in 5.0 mL of anhydrous acetonitrile. After the addition was completed, stirring was continued at room temperature until the end of the reaction. The reaction mixture was quenched with water (3.0 mL). The mixture was extracted with dichloromethane (10.0 mL). The organic layer was separated and washed with saturated sodium bicarbonate solution (3 × 10.0 mL), saturated brine (2 × 10.0 mL), and then dried over anhydrous magnesium sulfate. The solvent was removed under vacuum and the resulting mixture was dissolved in boiling ethyl acetate (1.0 mL) that, upon cooling, resulted in a red to yellow solid. This solid was recrystallized in ethyl acetate to obtain a yellow to off-white solid, depending on the product.

*2.3.1.1. 1,2,4,5-Tetra-p-tolyl-1,4-dihydro-pyrrolo[3,2-b]pyrrole (**4aaa**).* RMN-^1H (400 MHz, $CDCl_3$): δ(ppm) 7.19–7.16 (m, 8H), 7.11 (d, J = 8.1 Hz, 4 H), 7.03 (d, J = 8.3 Hz, 4H), 6.33 (s, 2H), 2.36 (s, 6H), 2.30 (s, 6H). RMN-^{13}C (100 MHz, $CDCl_3$): δ(ppm) 137.7 (2C), 135.7 (2C), 135.6 (2C), 135.1 (2C), 131.3 (2C), 131.0 (2C), 129.6 (4CH), 128.8 (4CH), 128.1 (4CH), 125.1 (4CH), 94.1 (2CH), 21.1 ($2CH_3$), 21.0 ($2CH_3$). IR (ν_{max}/cm^{-1}): 1734, 1610, 1513, 1475, 1373, 1135, 816. ESI-HRMS: m/z calcd for $C_{34}H_{30}N_2$ $[M]^+$: 466.24090; found 466.2401.

*2.3.1.2. 2,5-Diphenyl-1,4-di-p-tolyl-1,4-dihydro-pyrrolo[3,2-b]pyrrole (**4baa**).* RMN-^1H (400 MHz, $CDCl_3$): δ(ppm) 7.22 (d, J = 4.5 Hz, 10H), 7.16 (d, J = 3.3 Hz, 8H), 6.38 (s, 2H), 2.37 (s, 6H). RMN-^{13}C (100 MHz, $CDCl_3$): δ(ppm) 137.6 (2C), 135.7 (2C), 135.3 (2C), 133.8 (2C), 131.6 (2C), 129.7 (4CH), 128.2 (4CH), 128.1 (4CH), 126.0 (2CH), 125.1 (4CH), 94.5 (2CH), 21.0 ($2CH_3$). IR (ν_{max}/cm^{-1}): 1596, 1515, 1470, 1383, 1141, 826. ESI-HRMS: m/z calcd for $C_{32}H_{26}N_2$ $[M]^+$: 438.20960; found 438.1365.

*2.3.1.3. 2,5-Bis-(4-methoxy-phenyl)-1,4-di-p-tolyl-1,4-dihydro-pyrrolo[3,2-b]pyrrole (**4caa**).* RMN-^1H (400 MHz, $CDCl_3$): δ(ppm) 7.16–7.13 (m, 12H), 6.77 (d, J = 8.8 Hz, 4H), 6.29 (s, 2H), 3.78, (s, 6H), 2.36 (s, 6H). RMN-^{13}C (100 MHz, $CDCl_3$): δ(ppm) 158.1 (2C), 137.7 (2C), 135.2 (2C), 135.1 (2C), 130.9 (2C), 129.6 (4CH), 129.5 (4CH), 126.7 (2C), 125.0 (4CH), 113.6 (4CH), 93.7 (2CH), 55.2 ($2CH_3$), 21.0 ($2CH_3$). IR (ν_{max}/cm^{-1}): 1607, 1554, 1478, 1322, 1176, 1053, 798. ESI-HRMS: m/z calcd for $C_{34}H_{30}N_2O_2$ $[M]^+$: 498.23073; found 498.1479.

*2.3.1.4. 2,5-Bis-(4-chloro-phenyl)-1,4-di-p-tolyl-1,4-dihydro-pyrrolo[3,2-b]pyrrole (**4daa**).* RMN-^1H (400 MHz, $CDCl_3$): δ(ppm) 7.19–7.12 (m, 16H), 6.35 (s, 2H), 2.38 (s, 6H). RMN-^{13}C (100 MHz, $CDCl_3$): δ(ppm) 137.2 (2C), 135.8 (2C), 134.8 (2C), 132.2 (2C), 131.9 (2C), 131.8 (2C), 129.9 (4CH), 129.2 (4CH), 128.4 (4CH), 125.1 (4CH), 94.6 (2CH), 21.0 ($2CH_3$). IR (ν_{max}/cm^{-1}): 1513, 1466, 1410, 1374, 1089, 828, 546, 505. ESI-HRMS: m/z calcd for $C_{32}H_{24}Cl_2N_2$ $[M]^+$: 506.13165; found 506.1319.

*2.3.1.5. 2,5-Bis-(4-bromo-phenyl)-1,4-di-p-tolyl-1,4-dihydro-pyrrolo[3,2-b]pyrrole (**4eaa**).* RMN-^1H (400 MHz, $CDCl_3$): δ(ppm) 7.33 (d, J = 8.3 Hz, 4H), 7.19–7.13 (m, 8H), 7.07 (d, J = 8.6 Hz, 4H), 6.35 (s, 2H), 2.38 (s, 6H). RMN-^{13}C (100 MHz, $CDCl_3$): δ(ppm) 137.2 (2C), 135.8 (2C), 134.8 (2C), 132.6 (2C), 132.0 (2C), 131.3 (4CH), 129.9 (4CH), 129.5 (4CH), 125.1 (4CH), 120.0 (2C), 94.6 (2CH), 21.0 ($2CH_3$). IR (ν_{max}/cm^{-1}): 1513, 1466, 1372, 1135, 1009, 819, 539. ESI-HRMS: m/z calcd for $C_{32}H_{24}Br_2N_2$ $[M]^+$: 594.03062; found 594.0309.

*2.3.1.6. 2,5-Bis-(4-tert-butyl-phenyl)-1,4-di-p-tolyl-1,4-dihydro-pyrrolo[3,2-b]pyrrole (**4faa**).* RMN-^1H (400 MHz, $CDCl_3$): δ(ppm) 7.23 (d, J = 8.6 Hz, 4H), 7.19 (d, J = 8.6 Hz, 4H), 7.15 (d, J = 2.3 Hz, 4H), 7.13 (d, J = 2.0 Hz, 4H), 6.34 (s, 2H), 2.38 (s, 6H), 1.29 (s, 9H). IR (ν_{max}/cm^{-1}): 2960, 1607, 1513, 1461, 1413, 1362, 1267, 1142, 829, 762. ESI-HRMS: m/z calcd for $C_{40}H_{42}N_2$ $[M]^+$: 550.33480; found 550.3344.

*2.3.1.7. 2,5-Bis-(4-methylsulfanyl-phenyl)-1,4-di-p-tolyl-1,4-dihydro-pyrrolo[3,2-b]pyrrole (**4gaa**).* RMN-^1H (400 MHz, $CDCl_3$): δ(ppm) 7.15–7.09 (m, 16H), 6.34 (s, 2H), 2.46 (s, 6H), 2.37 (s, 6H). RMN-^{13}C (100 MHz, $CDCl_3$): δ(ppm) 137.5 (2C), 135.9 (2C), 135.4 (2C), 135.3 (2C), 131.7 (2C), 130.7 (2C), 129.8 (4CH), 128.4 (4CH), 126.3 (4CH), 125.1 (4CH), 94.2 (2CH), 21.0 ($2CH_3$), 15.9 ($2CH_3$). IR (ν_{max}/cm^{-1}): 1512, 1466, 1410, 1373, 1139, 1097, 822, 753. ESI-HRMS: m/z calcd for $C_{34}H_{30}N_2S_2$ $[M]^+$: 530.18504; found 530.1954.

*2.3.1.8. 2,5-Bis-biphenyl-4-yl-1,4-di-p-tolyl-1,4-dihydro-pyrrolo[3,2-b]pyrrole (**4haa**).* RMN-^1H (400 MHz, $CDCl_3$): δ(ppm) 7.59 (d, J = 8.3 Hz, 5H), 7.48 (d, J = 8.3 Hz, 5H), 7.33–7.29 (m, 8H), 7.24 (d, J = 8.3 Hz, 4H), 7.19 (d, J = 8.6 Hz, 4H), 6.44 (s, 2H), 2.39 (s, 6H). IR

(ν_{max}/cm^{-1}): 1604, 1514, 1470, 1378, 1140, 843, 756. ESI-HRMS: *m/z* calcd for $C_{44}H_{34}N_2$ $[M]^+$: 590.27220; found 590.2719.

*2.3.1.9. 1,4-Bis-(4-bromo-phenyl)-2,5-di-p-tolyl-1,4-dihydro-pyrrolo [3,2-b]pyrrole (**4aba**).* RMN-^{1}H (400 MHz, $CDCl_3$): δ(ppm) 7.46 (d, *J* = 8.9 Hz, 4H), 7.14 (d, *J* = 8.6 Hz, 4H), 7.08 (q, J_1 = 8.4 Hz, J_2 = 5.6 Hz, 8H), 6.34 (s, 2H), 2.33 (s, 6H). RMN-^{13}C (100 MHz, $CDCl_3$): δ(ppm) 139.1 (2C), 136.3 (2C), 135.8 (2C), 132.2 (4CH), 131.0 (2C), 130.4 (2C), 129.1 (4CH), 128.2 (4CH), 126.6 (4CH), 118.9 (2C), 94.9 (2CH), 21.2 ($2CH_3$). IR (ν_{max}/cm^{-1}): 1586, 1530, 1489, 1401, 1373, 1134, 1072, 1008, 825, 765, 476. ESI-HRMS: *m/z* calcd for $C_{32}H_{24}Br_2N_2$ $[M]^+$: 594.03062; found 594.0303.

*2.3.1.10. 1,4-Bis-(4-methoxy-phenyl)-2,5-di-p-tolyl-1,4-dihydro-pyrrolo[3,2-b]pyrrole (**4aca**).* RMN-^{1}H (400 MHz, $CDCl_3$): δ(ppm) 7.21 (d, *J* = 8.8 Hz, 4H), 7.10 (d, *J* = 8.3 Hz, 4H), 7.02 (d, *J* = 8.3 Hz, 4H), 6.88 (d, *J* = 8.8 Hz, 4H), 6.30 (s, 2H), 3.82 (s, 6H), 2.30 (s, 2H). RMN-^{13}C (100 MHz, $CDCl_3$): δ(ppm) 157.4 (2C), 135.8 (2C), 135.6 (2C), 133.4 (2C), 131.5 (2C), 131.0 (2C), 128.9 (4CH), 128.0 (4CH), 126.6 (4CH), 114.3 (4CH), 93.5 (2CH), 55.4 ($2CH_3$), 21.1 ($2CH_3$). IR (ν_{max}/cm^{-1}): 1514, 1442, 1294, 1246, 1028, 822, 752. ESI-HRMS: *m/z* calcd for $C_{34}H_{30}N_2O_2$ $[M]^+$: 498,23073; found 498.2311.

*2.3.1.11. 2,5-Bis-(4-fluoro-phenyl)-1,4-bis-(4-methoxy-phenyl)-1,4-dihydro-pyrrolo[3,2-b]pyrrole (**4ica**).* RMN-^{1}H (400 MHz, $CDCl_3$): δ(ppm) 7.20–7.15 (m, 8H), 6.94–6.88 (m, 8H), 6.29 (s, 2H), 3.83 (s, 6H). RMN-^{13}C (100 MHz, $CDCl_3$): δ(ppm) 162.7 (2C), 160.2 (2C), 157.7 (2C), 134.9 (2C), 133.0 (2C), 131.4 (2C), 129.8 (2CH), 129.7 (2CH), 126.6 (4CH), 115.2 (2CH), 115.0 (2CH), 114.4 (4CH), 93.6 (2CH), 55.5 ($2CH_3$). IR (ν_{max}/cm^{-1}): 1514, 1460, 1296, 1250, 1213, 1032, 837, 767. ESI-HRMS: *m/z* calcd for $C_{32}H_{24}F_2N_2O_2$ $[M]^+$: 506.18058; found 506.1804.

*2.3.1.12. 1,4-Diphenyl-2,5-di-p-tolyl-1,4-dihydro-pyrrolo[3,2-b]pyrrole (**4ada**).* RMN-^{1}H (400 MHz, $CDCl_3$): δ(ppm) 7.34 (d, *J* = 7.3 Hz, 5H), 7.29 (d, *J* = 7.3 Hz, 5H), 7.11 (d, *J* = 8.1 Hz, 4H), 7.03 (d, *J* = 8.1 Hz, 4H), 6.38 (s, 2H), 2.31 (s, 6H). RMN-^{13}C (100 MHz, $CDCl_3$): δ(ppm) 140.2 (2C), 135.9 (2C), 135.7 (2C), 131.3 (2C), 130.9 (2C), 129.0(4CH), 128.9(4CH), 128.1 (4CH), 125.5 (2CH), 125.2 (4CH), 94.6 (2CH), 21.1 ($2CH_3$). IR (ν_{max}/cm^{-1}): 1595, 1498, 1433, 1371, 1130, 816, 751, 694. ESI-HRMS: *m/z* calcd for $C_{32}H_{26}N_2$ $[M]^+$: 438.20960; found 438.2095.

*2.3.1.13. Methyl 4-{2,4,5-tris[4-(methoxycarbonyl)phenyl]pyrrolo [3,2-b]pyrrol-1-yl}benzoate (**4jea**).* RMN-^{1}H (400 MHz, $CDCl_3$): δ(ppm) 8.06 (d, *J* = 8.8 Hz, 4H), 7.91 (d, *J* = 8.6 Hz, 4H), 7.32 (d, *J* = 8.6 Hz, 4H), 7.27 (d, *J* = 8.6 Hz, 4H), 6.56 (s, 2H), 3.94 (s, 6H), 3.90 (s, 6H). RMN-^{13}C (100 MHz, $CDCl_3$): δ(ppm) 166.8 (2C), 166.3 (2C), 143.4 (2C), 137.3 (2C), 135.8 (2C), 132.5 (2C), 130.9 (4CH), 129.7 (4CH), 128.0 (2C), 127.7 (4CH), 124.6 (4CH), 97.3 (2CH), 52.2 ($2CH_3$), 52.1 ($2CH_3$). IR (ν_{max}/cm^{-1}): 1727, 1685, 1577, 1502, 1437, 1391, 1284, 1203, 1107, 1013, 851, 809, 757, 686. ESI-HRMS: *m/z* calcd for $C_{38}H_{30}N_2O_8$ $[M]^+$: 642.20022; found 642.2007.

3. Results and discussion

3.1. Synthetic studies

The optimization studies of the synthesis of tetraaryl-1,4-dihydropyrrolo-[3,2-*b*]pyrrole derivatives by MCR were made using tolualdehyde (**1a**), toluidine (**2a**) and 2,3-butanodione (**3a**) in different solvents and varying the proportions of $NbCl_5$ catalyst (Scheme 2 and Table 1). From these tests, the best conditions obtained were those using acetonitrile as solvent and the proportion of 0.250 mmol of $NbCl_5$ as catalyst. It is interesting to note that no product formation is observed in the acetic acid-based systems, differently from the systems containing $NbCl_5$. Another noteworthy result is that a high concentration of $NbCl_5$ (more than 0.250 mmol) does not improve the reaction yield, probably due to the formation of by-products during the synthesis.

Based on these results, several reactions involving different benzaldehyde derivatives (**1a-j**), aniline derivatives (**2a-e**) and β-diketone derivatives (**3a-c**) in the presence of 0.250 mmols of $NbCl_5$ and using MeCN as solvent were performed (see Scheme 3). The obtained results are shown in Table 2.

Note that the substituents in *para* position of benzaldehyde or aniline have small effects on the reaction yields or on their completion times. In general, reactions employing **3b** and **3c** β-diketones do not lead to the formation of the desired products. These results can be associated with sterical hindrance in the second Schiff base attack due to the presence of alkyl groups in **3b** and **3c** diketones, which prevents the formation of tetraaryl-1,4-

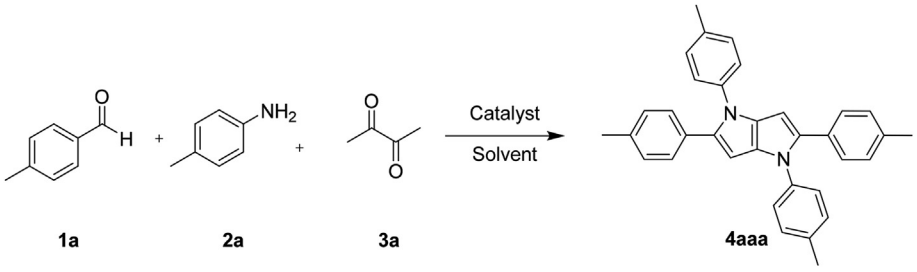

Scheme 2. Optimization reaction tests.

Table 1
Optimization tests results.

Entry	Solvent	$NbCl_5$ amount (mmol)	Yield (%)	Reaction time (min)
1	Acetic acid	0.250	–	120
2	Dichloromethane	0.250	50	50
3	Acetonitrile	0.125	70	40
4	Acetonitrile	0.250	82	20
5	Acetonitrile	0.500	82	10
6	Acetonitrile	1.000	65	10

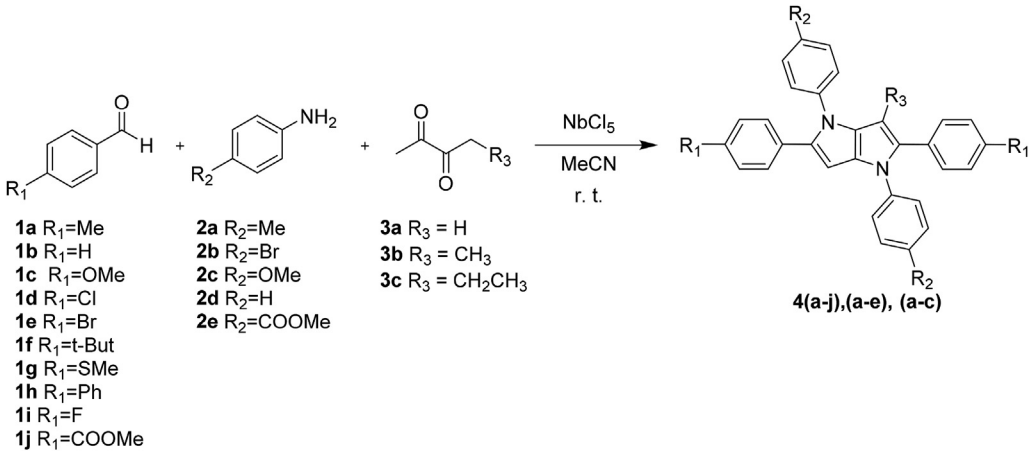

Scheme 3. MCR using aniline, benzaldehyde and β-diketone derivatives in the presence of $NbCl_5$, as catalyst.

Table 2
Results of the synthesis of tetraaryl-1,4-dihydropyrrolo-[3,2-*b*]pyrrole derivatives by MRCs using $NbCl_5$.

Entry	Benzaldehyde derivative	Aniline derivative	β-diketone	Yield (%)	Reaction time (min)
1	**1a**	**2a**	**3a**	82 (**4aaa**)	20
2	**1b**	**2a**	**3a**	85 (**4baa**)	20
3	**1c**	**2a**	**3a**	98 (**4caa**)	20
4	**1d**	**2a**	**3a**	95 (**4daa**)	40
5	**1e**	**2a**	**3a**	92 (**4eaa**)	30
6	**1f**	**2a**	**3a**	73 (**4faa**)	20
7	**1g**	**2a**	**3a**	98 (**4gaa**)	40
8	**1h**	**2a**	**3a**	83 (**4haa**)	40
9	**1a**	**2b**	**3a**	80 (**4aba**)	40
10	**1a**	**2c**	**3a**	77 (**4aca**)	40
11	**1i**	**2c**	**3a**	59 (**4ica**)	40
12	**1a**	**2d**	**3a**	68 (**4ada**)	20
13	**1j**	**2e**	**3a**	96 (**4jea**)	40
14	**1i**	**2a**	**3b**	– (**4iab**)	120
15	**1a**	**2a**	**3c**	– (**4aac**)	120
16	**1h**	**2a**	**3b**	– (**4hab**)	120
17	**1a**	**2b**	**3b**	– (**4abb**)	120
18	**1i**	**2b**	**3c**	– (**4ibc**)	120

dihydropyrrolo-[3,2-*b*]pyrrole derivatives. Fig. 1 illustrates the difference in the volume of these compounds (data coming from electronic structure calculations) reinforcing this hypothesis.

Comparing the results obtained in this work with others found in the literature (Table 3), it is possible to verify the effectiveness of $NbCl_5$ as catalyst in the synthesis of tetraaryl-1,4-dihydropyrrolo [3,2-*b*]pyrrole derivatives [41,42].

The results show that niobium pentachloride can be considered an efficient catalyst in comparison with other Lewis acids (regarding reaction time and yield).

It is worth mentioning that compounds **4aca** are obtained only in $NbCl_5$ catalyzed reactions. We believe that the great oxophilicity of niobium pentachloride explains that result, since the $NbCl_5$ can bond to the oxygen of the methoxy group in the 4-anisaldehyde, thus stabilizing the molecule, which does not occur in the presence of the acetic acid.

In order to better understand some essential features of the mechanisms involved in the synthesis of tetraaryl-1,4-dihydropyrrolo[3,2-*b*]pyrrole derivatives, the local softness of each of the **1**, **2** and **3** components were calculated. The tendency of atoms interactions was evaluated via HSAB (hard-soft acid-base) principle.

The local softness (s^+ and s^-) was obtained via Condensed-to-atoms Fukui indexes (CAFI). Despite being obtained via a very simplified approach, these descriptors have been successfully employed to understand and predict reactivity features of distinct molecules and polymers [63–67]. Given the nature of the involved reactions, only CAFIs associated with nucleophilic (f^+) and electrophilic (f^-) agents were calculated.

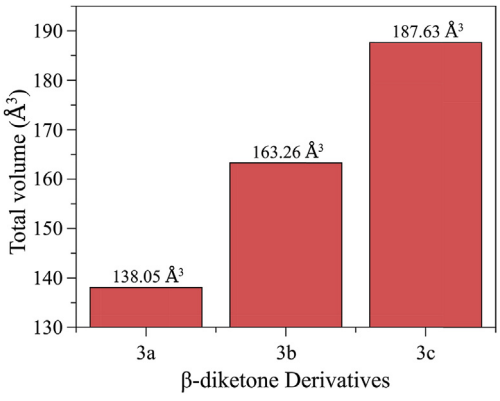

Fig. 1. Total volume of **3a**, **3b** and **3c** β-diketones.

Table 3
Comparison between the results presented in this report and the ones found in the literature.

Product	Lewis acid	Catalyst proportion (%)	Time (min)	Yield (%)
4aaa	**$NbCl_5$**	**12.5**[a]	**20**	**82**
4aaa	AcOH	Solvent	210	34
4aaa	TsOH	10	210	34
4baa	**$NbCl_5$**	**12.5**[a]	**20**	**85**
4baa	AcOH	Solvent	210	33
4baa	TsOH	10	210	34
4caa	**$NbCl_5$**	**12.5**[a]	**20**	**98**
4caa	AcOH	Solvent	210	15
4aba	**$NbCl_5$**	**12.5**[a]	**40**	**80**
4aba	AcOH	Solvent	210	15
4aba	TsOH	10	210	22
4aca	**$NbCl_5$**	**12.5**[a]	**40**	**77**
4aca	AcOH	Solvent	210	–
4ica	**$NbCl_5$**	**12.5**[a]	**40**	**59**
4ica	AcOH	Solvent	210	07

[a] 0.250 mmols of $NbCl_5$ were used, corresponding to 12.5 mol% to the aniline derivative used.

$$f_i^+ = q_i(N+1) - q_i(N) \quad (2)$$

$$f_i^- = q_i(N) - q_i(N-1) \quad (3)$$

where $q_i(N+1)$, $q_i(N)$ and $q_i(N-1)$ represent the electronic population in the *i*-th atom of anionic, cationic and neutral species of the system under study, respectively. The Hirshfeld partition method was employed to estimate the electronic populations in order to avoid negative CAFI values [68].

The electronic descriptors s^+ and s^- were obtained from the multiplication of CAFIs with the global softness of the compounds ($S = 1/(IP\text{-}EA)$):

$$s_i^k = S f_i^k, \quad \text{for } k = + \text{ or } - \quad (4)$$

where *IP* and *EA* represent, respectively, the ionization potential and the electron affinity of the species estimated via Eqs. (5) and (6).

$$IP = E(N-1) - E(N), \quad (5)$$

$$EA = E(N) - E(N+1), \quad (6)$$

with *E(M)* representing the total energy of the chemical species with *M* electrons.

According to the HSAB principle, electrophile/nucleophile interactions are favored when the involved atoms present similar softness [69,70]. In this sense, it was possible to propose specific reactions occurring during the synthesis process.

Fig. 2 illustrates the local softness of *i)* compound **1** for reactions toward nucleophiles (s^+) and *ii)* compounds **2** and **3** for reactions toward electrophiles (s^-).

As it can be noticed, the interaction between C_7 of compound **1** (yellow circle) and N_7 of compound **2** (yellow square) is favored, given the major similarity of the relative softness of these atoms. An effective interaction between these sites leads to the formation of specific intermediates, which are necessary for the production of tetraaryl-1,4-dihydropyrrolo[3,2-*b*]pyrrole derivatives (see Scheme 1). However, the results presented in Fig. 2 indicate that effective interactions can also occur between C_7 of compound **1** (yellow circles) and oxygen atoms of compound **3** (cyan and yellow triangles), suggesting a possible competing route for the formation of compounds **4** that could explain the small yield differences presented in Table 3.

Fig. 3 illustrates the correlation between $ln(\left|s^+_{1(C_7)} - s^-_{3(O_5/O_7)}\right|)$ (that is a measure of the difference between the local softness of the C_7 of compound **1** and O_5, or O_7, of compound **3**) and the experimental yields. It is possible to observe that a linear relation is obtained, indicating that systems with lower probability of direct interactions between compounds **1** and **3** present higher yields, which is compatible with the mechanism proposed in Scheme 2. Compound **4ica** was identified as a possible outlier, which can be associated with the higher proximity between the s^- indexes of N_7 of compound **2c** and O_5 (O_7) of compound **3** (in comparison with **2a**, **2b**, **2d** and **2e**).

These results suggest that there are two competing mechanisms occurring during the synthesis process related to the interaction between C_7 of compound **1** and N_7 of compound **2** (a desired route) and C_7 of compound **1** and O_5 (or O_7) of compound **3** (undesired one). The balance between these routes can be (at some degree) adjusted by an appropriate choice of $\mathbf{R_1}$ and $\mathbf{R_2}$ ligands (excluding steric effects). Additional linear regressions reinforce this hypothesis (see Supplementary Information for details).

3.2. Photophysical studies

Considering the potential applications of tetraaryl-1,4-dihydropyrrolo-[3,2-b] pyrroles in organic electronics, a preliminary photo-physical characterization of the obtained compounds was performed. The optical properties were evaluated in dichloromethane and in the UV–Vis region. Figs. 4 and 5, and Table 4 present the main results obtained.

Most of the compounds present significant absorbance between 294 and 382 nm, suggesting that these materials can be employed as sensitizing dyes in optoelectronic devices.

In general, it is possible to observe that the presence of the chlorine, bromine and phenyl groups in the benzaldehyde *p*-position leads to a bathochromic effect in the spectra. Such red-shift can be associated with the extension of the conjugation length promoted by the presence of the phenyl group, as well as halogen inductive effects that stabilize the excited state. On the other hand, a small hypsochromic shift is observed in the spectra when the fluorine group is present in aniline, and methoxy is present in the benzaldehyde derivative. Such effect can be associated with the strong electronegative effect induced by the fluorine atom that, in turn, destabilizes the excited state.

Regarding fluorescence, it is observed that most of the compounds present maximum emission, about 420 nm. Compounds **4haa** and **4aba** present the highest red shift, with the main emission peak close to 460 nm for both products. In relation to the quantum yields, it is observed that compounds **4caa**, **4eaa**, **4aba** and **4jea** present very low efficiencies ($\Phi < 0.1$), while compounds **4daa**, **4gaa** and **4haa** present the highest values ($\Phi > 0.8$). The low Φ values associated with compounds containing bromine atoms (**4eaa** and **4aba**) can be associated to the heavy atom effect [71], however such effect is not present in chlorine-containing systems (**4daa**).

In order to better evaluate the transitions involved, theoretical absorption spectra were carried out for all the products obtained (compounds **4aaa**–**4jea** are presented in Table 3). In addition, 90 new derivatives obtained from varied combinations of distinct $\mathbf{R_1}$ (H, 4-CH_3, Br, Cl, 4-OCH_3, 4-NO_2) and $\mathbf{R_2}$ (H; 4-Cl; 4-Br; 4-F; 4-NO_2; 4-OCH_3; 4-CH_3; 4-$C(CH_3)_3$; 4-$N(CH_3)_2$; 4-SCH_3; 4-Ph 2,4-OH; 3-OCH_3; 4-OH; 2,4,6-CH_3) ligands were evaluated so as to propose compounds with improved optoelectronic properties.

The theoretical absorption spectra of the compounds were calculated in a time-dependent DFT (TD-DFT) approach with B3LYP functional and 6-311G(d,p) basis set. The presence of the solvent

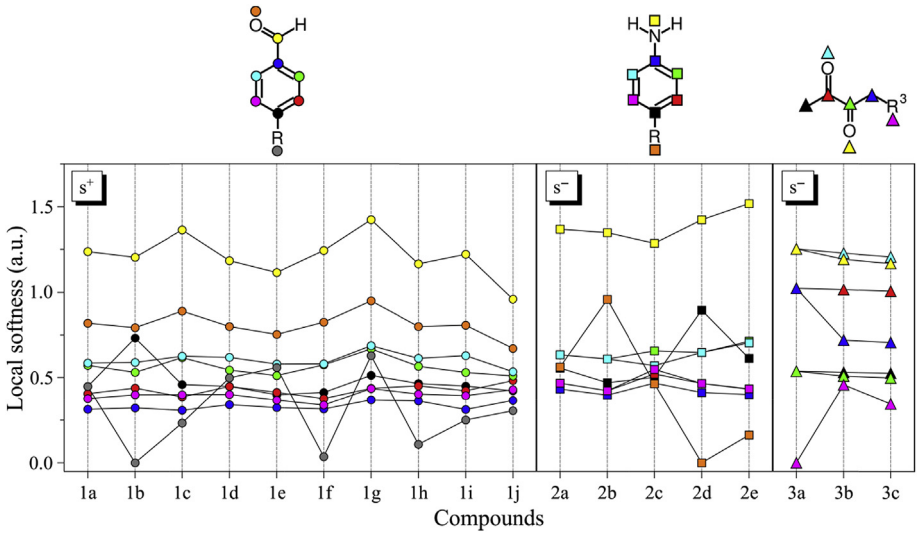

Fig. 2. Local softness of compounds **1** (s^+), **2** (s^-) and **3** (s^-).

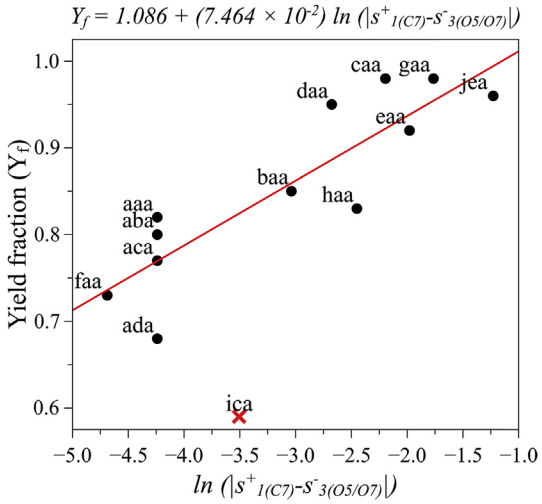

Fig. 3. Correlation between total yields and the similarity between the local softness of C_7 of compound **1** and O_5 (or O_7) of compound **3**.

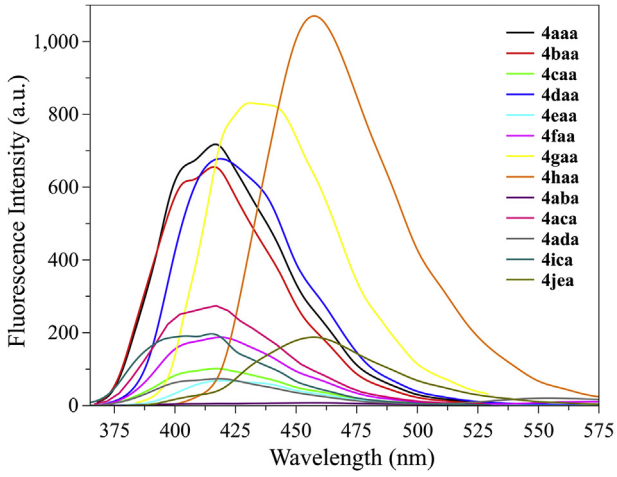

Fig. 5. Fluorescence spectra of the studied compounds.

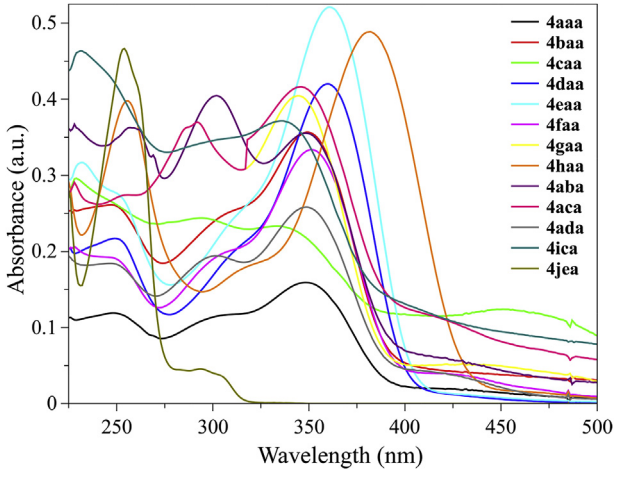

Fig. 4. UV–Vis absorption spectra of the studied compounds.

Table 4
Summary of the main optical data of the compounds.

Compound	λ_{abs} (nm)	λ_{emi} (nm)	Stokes shift (nm)	ε (L.M^{-1}.cm^{-1})	Φ^a
4aaa	348	418	70	$1,6 \times 10^5$	0.45
4baa	349	418	69	$3,6 \times 10^5$	0.56
4caa	343	418	75	$2,3 \times 10^5$	0.07
4daa	360	420	60	$4,2 \times 10^5$	0.83
4eaa	361	420	59	$5,2 \times 10^5$	0.06
4faa	351	420	69	$3,3 \times 10^5$	0.11
4gaa	344	434	90	$4,0 \times 10^5$	0.87
4haa	382	460	78	$4,9 \times 10^5$	0.90
4aba	348	460	112	$3,5 \times 10^5$	0.03
4aca	346	417	71	$4,2 \times 10^5$	0.22
4ica	336	415	79	$3,7 \times 10^5$	0.42
4ada	349	420	71	$2,6 \times 10^5$	0.38
4jea	294	430	136	$4,6 \times 10^4$	0.03

[a] Determined using 9,10-diphenylanthracene in ethanol ($1,0 \times 10^{-5}$ M) as standard.

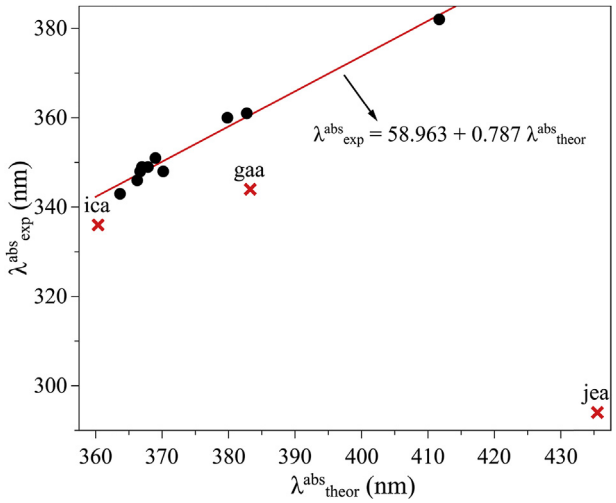

Fig. 6. Relationship between theoretical and experimental optical absorption main peak position of the compounds. The linear fit is based only on the black points. Red points were identified as possible outliers. (For interpretation of the references to colour in this figure legend, the reader is referred to the web version of this article.)

(CH_2Cl_2) was simulated using the PCM. All the calculations were performed with the aid of the Gaussian computational package [62].

Fig. 6 illustrates the relation between experimental and predicted optical absorption main peak position. As it can be noticed, a linear relationship is observed for most derivatives. Compound **4jea** was identified as a possible outlier. Compounds **4ica** and **4gaa** present not so dissonant results.

The absorption spectra of the compounds are in general composed by two or three main peaks (see Fig. 4) that can be associated with π-π* transitions (see Supplementary Information). It is noticed that the presence of the distinct ligands changes the balance between the amplitude of these peaks. Particularly, the spectrum of the **4jea** compound does not present the transition at higher wavelengths, which can suggest possible problems in the formation of an extended π-conjugated system during the synthesis process.

Fig. 7 illustrates the most relevant Kohn-Sham orbitals involved in the main optical transitions of the compound **4aaa**. HOMO, LUMO, HOMO-*n* and LUMO-*m* represent, respectively, the highest occupied molecular orbital, the lowest unoccupied molecular orbital, the *n*-th energy level below the HOMO and the *m*-th energy level above the LUMO. Very similar results were obtained for the other 12 compounds and are presented in detail in the Supplementary Information.

As it can be observed, the main absorption peak is associated with a HOMO→LUMO (H-L) transition. In this context, given the HOMO distribution and the high relative oscillator strength (f_{osc}) of H-L transition, it is possible to consider that the optical responses of compounds **4** are more highly regulated by substitutions in $\mathbf{R_1}$ than in $\mathbf{R_2}$. Secondary significant transitions involving HOMO-1→LUMO (H1-L) and HOMO→LUMO+4 (H-L4) are also observed, which in some cases involve orbitals located at the aniline-based ring ($\mathbf{R_2}$ ring). However, the associated f_{osc} values are quite small for these transitions, indicating that they have no significant effect on the overall spectra.

Despite of being very difficult to interpret the varied factors that can influence the photoluminescence of the compounds in solution, the analysis of Fig. 7 and Figs. S2–S13 (see Supplementary Information) suggest that the obtained quantum yields depends on the spatial distribution of the LUMO on the structure of the compounds. In general it is observed that compounds with low quantum yields present a significant part of the LUMO located on the $\mathbf{R_2}$ rings. This feature are more evident in the compounds with very low quantum yields, as **4caa**, **4aba** and **4jea** (with an exception to compound **4eaa** in which heavy atom effect apparently dominates the optical response) and it is absent in compounds with the highest yields (**4daa**, **4gaa** and **4haa**) and could be associated with non-radiative routes. However, more studies are still necessary for an in deep analysis, which are not in the scope of the present work.

Aiming at better evaluating the influence of the ligands on the optical properties of tetraaryl-1,4-dihydropyrrolo-[3,2-*b*]pyrroles, the optical absorption spectra of 90 distinct derivatives were (only theoretically) assessed. These compounds were designed considering typical substitutions that could be promoted in $\mathbf{R_1}$ and $\mathbf{R_2}$ positions ($\mathbf{R_1}$ = H, 4-CH_3, Br, Cl, 4-OCH_3, 4-NO_2/$\mathbf{R_2}$ = H; 4-Cl; 4-Br; 4-F; 4-NO_2; 4-OCH_3; 4-CH_3; 4-$C(CH_3)_3$; 4-$N(CH_3)_2$; 4-SCH_3; 4-Ph 2,4-OH; 3-OCH_3; 4-OH; 2,4,6-CH_3). Fig. 8 illustrates the influence of each ligand, $\mathbf{R_1}$ and $\mathbf{R_2}$, on the main peak position of the derivatives (details regarding the optical properties of these

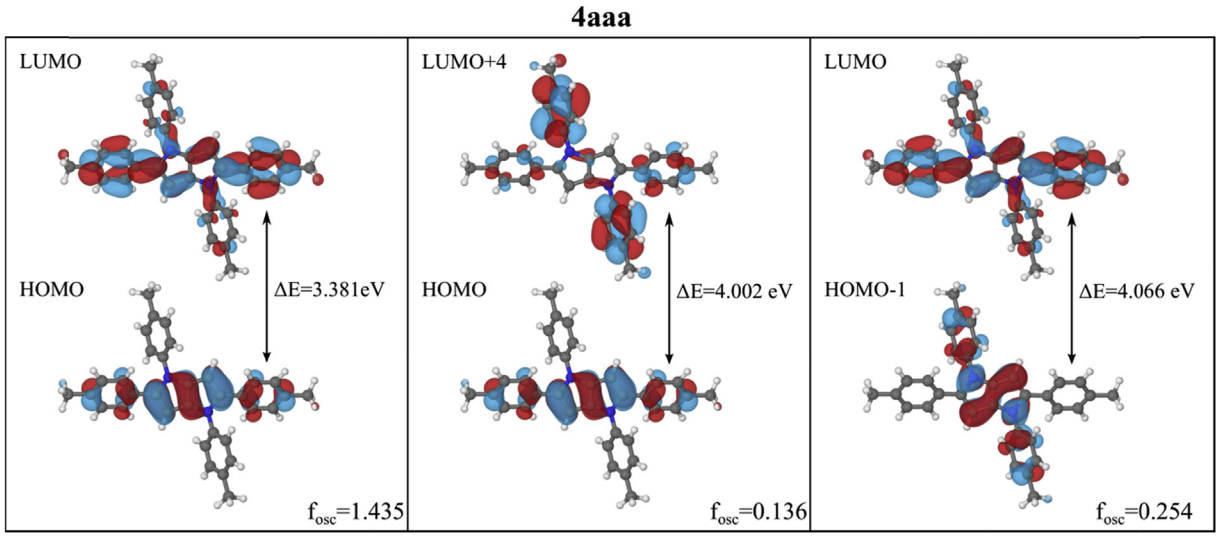

Fig. 7. Relevant Kohn-Sham orbitals involved in the main optical transitions of the compound **4aaa**.

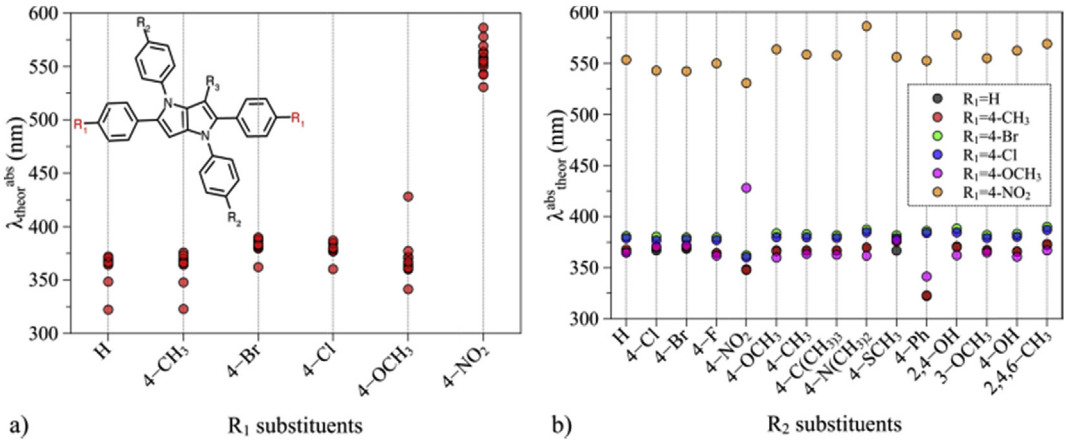

Fig. 8. Influence of the $\mathbf{R_1}$ (a) and $\mathbf{R_2}$ (b) substituents on the main peak position of the tetraaryl-1,4-dihydropyrrolo-[3,2-*b*]pyrrole derivatives absorption spectra.

compounds can be found in the Supplementary Information).

The results reinforce our previous considerations, indicating that the main optical properties of the derivatives are indeed related to the $\mathbf{R_1}$ substituent. In particular, absorptions in the range of 500–600 nm are observed for $\mathbf{R_1}$ = NO_2, while absorptions at lower wavelengths are observed for $\mathbf{R_1}$ = H and 4-CH_3. Very weak dependence on the nature of $\mathbf{R_2}$ substituent is observed. In general, absorptions at lower wavelengths are obtained for $\mathbf{R_2}$ = 4-Ph, while $\mathbf{R_2}$ = NO_2 leads to absorptions at higher wavelengths than when $\mathbf{R_1}$ = OCH_3.

These results suggest that compounds with improved optical properties can be obtained via an appropriate choice of $\mathbf{R_1}$ substituents. Additional statistical studies are currently underway in order to propose and test guided routes for the production of materials with improved optoelectronic properties.

4. Conclusions

The objective of the present study was to show a new methodology for the synthesis of tetraaryl-1,4-dihydropyrrolo[3,2-*b*]pyrrole derivatives by a MCR between benzaldehyde, aniline and butane-2,3-dione derivatives, promoted by niobium pentachloride. Excellent yields and low reaction times were obtained under mild conditions. Electronic structure calculations indicate the existence of competing mechanisms occurring during the synthesis process that can be modulated, in some degree, by an appropriate choice of the benzaldehyde and aniline derivatives.

The optical characterization of the obtained tetraaryl-1,4-dihydropyrrolo-[3,2-*b*]pyrrole derivatives point out that such compounds can be employed as sensitizer dyes in organic electronic devices [8,72]. By means of theoretical studies, it was possible to assess relevant information on the optical properties of these materials. Above all, it was possible to identify that the main features of the absorption spectra of tetraaryl-1,4-dihydropyrrolo-[3,2-*b*]pyrrole derivatives are controlled by the nature of the benzaldehyde derivatives employed in the MCR process.

Acknowledgements

The authors would like to acknowledge the Fundação de Amparo à Pesquisa do Estado de São Paulo (Proc. 16/01599-1), Conselho Nacional de Desenvolvimento Científico e Tecnológico (Proc. 302753/2015-0, Proc. 448310/2014-7), Coordenadoria de Aperfeiçoamento de Pessoal do Nível Superior (CAPES) and Pró-Reitoria de Pesquisa da UNESP (PROPe-UNESP, PROPe-UNESP-PIBIC-Reitoria-Proj. 40037) for their financial support. The authors would also like to thank the Companhia Brasileira de Metalurgia e Mineração (CBMM) for supplying the niobium pentachloride. This research was also supported by resources provided by the Center for Scientific Computing (NCC/GridUNESP) of São Paulo State University (UNESP).

Appendix A. Supplementary data

Supplementary data related to this article can be found at http://dx.doi.org/10.1016/j.dyepig.2017.08.056.

References

[1] Krutosíková A, Gracza T. Topics in heterocyclic chemistry. 2008.
[2] Biswas A, Das A, Ganguly B. New J Chem 2016;40:9304–12.
[3] McCulloch I, Heeney M, Chabinyc M, DeLongchamp D, Kline R, Cölle M, et al. Adv Mater 2009;21:1091–109.
[4] Roncali J. Chem Rev 1992;92:711–38.
[5] Jin Y, Kim K, Song S, Kim J, Kim J, Park S, et al. Bull Korean Chem Soc 2006;27:1043–7.
[6] Capan A, Veisi H, Goren A, Ozturk T. Macromolecules 2012;45:8228–36.
[7] Fuller L, Iddon B, Smith K. J Chem Soc Perkin Trans 1997;1:3465–70.
[8] Henssler J, Zhang X, Matzger A. J Org Chem 2009;74:9112–9.
[9] Kim J, Han A, Seo J, Oh J, Yang C. Chem Mater 2012;24:3464–72.
[10] Koh K, Wong-Foy A, Matzger A. J Am Chem Soc 2009;131:4184–5.
[11] Kuhn M, Falk F, Paradies J. Org Lett 2011;13:4100–3.
[12] Nenajdenko V, Sumerin V, Chernichenko K, Balenkova E. Org Lett 2004;6:3437–9.
[13] Orłowski R, Banasiewicz M, Clermont G, Castet F, Nazir R, Blanchard-Desce M, et al. Phys Chem Chem Phys 2015;17:23724–31.
[14] Friese D, Mikhaylov A, Krzeszewski M, Poronik Y, Rebane A, Ruud K, et al. Chem - A Eur J 2015;21:18364–74.
[15] Krzeszewski M, Kodama T, Espinoza E, Vullev V, Kubo T, Gryko D. Chem - A Eur J 2016;22:16478–88.
[16] Tanaka S, Kumagai T, Mukai T, Kobayashi T. Bull Chem Soc Jpn 1987;60:1981–3.
[17] Hayase F, Takahashi Y, Tominaga S, Miura M, Gomyo T, Kato H. Biosci Biotechnol Biochem 1999;63:1512–4.
[18] Sasaki S, Shirahashi Y, Nishiyama K, Watanabe H, Hayase F. Biosci Biotechnol Biochem 2006;70:2529–31.
[19] Shirahashi Y, Watanabe H, Hayase F. Biosci Biotechnol Biochem 2009;73:2287–92.
[20] Janiga A, Bednarska D, Thorsted B, Brewer J, Gryko D. Org Biomol Chem 2014;12:2874.
[21] Tasior M, Chotkowski M, Gryko D. Org Lett 2015;17:6106–9.
[22] Janiga A, Krzeszewski M, Gryko D. Chem - An Asian J 2014;10:212–8.
[23] Krzeszewski M, Gryko D. J Org Chem 2015;80:2893–9.
[24] Stężycki R, Grzybowski M, Clermont G, Blanchard-Desce M, Gryko D. Chem - A Eur J 2016;22:5198–203.
[25] Dereka B, Rosspeintner A, Krzeszewski M, Gryko D, Vauthey E. Angew Chem Int Ed 2016;55:15624–8.
[26] Krzeszewski M, Świder P, Dobrzycki L, Cyrański M, Danikiewicz W, Gryko D. Chem Commun 2016;52:11539–42.
[27] Tasior M, Gryko D. J Org Chem 2016;81:6580–6.

[28] Wu J, Yu C, Wen J, Chang C, Leung M. Anal Chem 2016;88:1195–201.
[29] Balasubramanyam RC, Kumar R, Ippolito S, Bhargava S, Periasamy S, Narayan R, et al. J Phys Chem C 2016;120:11313–23.
[30] Lee M, Kim J, Son HJ, Kim JY, Kim B, Kim H, et al. Sci Rep 2015;5.
[31] Fuse S, Sugiyama S, Maitani MM, Wada Y, Ogomi Y, Hayase S, et al. Chem – A Eur J 2014;20:10685–94.
[32] Liu X, Kong F, Guo F, Cheng T, Chen W, Yu T, et al. Dyes Pigments 2017;139:129–35.
[33] Holzer B, Bintinger J, Lumpi D, Choi C, Kim Y, Stöger B, et al. Chemphyschem 2017;18:549–63.
[34] Soldano C, D'Alpaos R, Generali G. ACS Photonics 2017;4:800–5.
[35] Noh Y, Kim D, Yoshida Y, Yase K, Jung B, Lim E, et al. Appl Phys Lett 2005;86:043501.
[36] Che X, Chung C, Liu X, Chou S, Liu Y, Wong K, et al. Adv Mater 2016;28:8248–55.
[37] Aratani T, Yoshihara H, Suzukamo G. Tetrahedron Lett 1989;30:1655–6.
[38] Kumagai T, Satake K, Kidoura K, Mukai T. Tetrahedron Lett 1983;24:2275–8.
[39] Kumagai T, Tanaka S, Mukai T. Tetrahedron Lett 1984;25:5669–72.
[40] Satake K, Kumagai T, Mukai T. Chem Lett 1984;13:2033–6.
[41] Janiga A, Glodkowska-Mrowka E, Stoklosa T, Gryko D. Asian J Org Chem 2013;2:411–5.
[42] Krzeszewski M, Thorsted B, Brewer J, Gryko D. J Org Chem 2014;79:3119–28.
[43] Wang R, Li B, Huang T, Shi L, Lu X. Tetrahedron Lett 2007;48:2071–3.
[44] Andrade CKZ. Curr Org Synth 2004;1:333–53.
[45] Andrade CKZ, Rocha R. Mini-Reviews Org Chem 2006;3:271–80.
[46] Hou J, Liu Y, Zhang Z. J Heterocycl Chem 2010:703–6.
[47] Hou J, Chen H, Zhang Z. Phosphorus, Sulfur, Silicon Relat Elem 2010;186:88–93.
[48] Hou J, Gao J, Zhang Z. Appl Organomet Chem 2010;25:47–53.
[49] Hou J, Gao J, Zhang Z. Monatsh für Chem 2011;142:495–9.
[50] Lacerda V, Santos DA, da Silva-Filho LC, Greco S, Santos RB. Aldrichimica Acta 2012;45:19–27.
[51] Arpini B, Bartolomeu AA, Andrade C, da Silva-Filho LC, Lacerda V. Curr Org Synth 2015;12:570–83.
[52] da Silva-Filho LC, da Silva BHST, Martins LM. Synlett 2012;23:1973–7.
[53] dos Santos WH, da Silva-Filho LC. Synthesis 2012;44:3361–5.
[54] Martins LM, da Silva BHST, Menezes ML, da Silva-Filho LC. Heterocycl Lett 2013;3:307–17.
[55] Andrade A, Santos GC, da Silva-Filho LC. J Heterocycl Chem 2014;52:273–7.
[56] Bartolomeu AA, Menezes ML, da Silva-Filho LC. Synth Commun 2015;45:1114–26.
[57] da Silva BHST, Martins LM, da Silva-Filho LC. Heterocycl Lett 2015;5:431–42.
[58] Oshiro PB, Lima PSSG, Menezes ML, da Silva-Filho LC. Tetrahedron Lett 2015;56:4476–9.
[59] Siqueira MS, da Silva-Filho LC. Tetrahedron Lett 2016;57:5050–2.
[60] Santos GC, Bartolomeu AA, Ximenes VF, da Silva-Filho LC. J Fluoresc 2016;27:271–80.
[61] dos Santos WH, da Silva-Filho LC. Tetrahedron Lett 2017;58:894–7.
[62] Frisch MJ, Trucks GW, Schlegel HB, Scuseria GE, Robb MA, Cheeseman JR, et al. Gaussian 09. Wallingford CT: Gaussian, Inc.; 2009.
[63] Mineva T. J Mol Struct Theochem 2006;762:79–86.
[64] Cruz J, Martínez-Aguilera LMR, Salcedo R, Castro M. Int J Quantum Chem 2001;85:546–56.
[65] Bronze-Uhle ES, Batagin-Neto A, Lavarda FC, Graeff CFO. J Appl Phys 2011;110:073510.
[66] Batagin-Neto A, Bronze-Uhle E, Vismara M, Assis A, Castro F, Geiger T, et al. Curr Phys Chem 2013;3:431–40.
[67] Cesarino I, Simões RP, Lavarda FC, Batagin-Neto A. Electrochimica Acta 2016;192:8–14.
[68] De Proft F, Van Alsenoy C, Peeters A, Langenaeker W, Geerlings P. J Comput Chem 2002;23:1198–209.
[69] Lewars EG. Computational chemistry: introduction to the theory and applications of molecular and quantum mechanics. second ed. Springer; 2010.
[70] Yang W, Mortier WJ. J Am Chem Soc 1986;108:5708–11.
[71] Valeur B, Berberan-Santos MN. Molecular fluorescence. second ed. Weinheim: VCH; 2012. p. 77.
[72] Dobrin S, Kaszynski P, Ikeda S, Waluk J. Chem Phys 1997;216:179–92.